Plant-Mediated Biological Synthesis of Ag-Ago-Ag_2O Nanocomposites Using Leaf Extracts of *Solanum Elaeagnifolium* for Antioxidant, Anticancer, and DNA Cleavage Activities

Mukul Barwant
Savitribai Phule Pune University
Yogesh Ugale
Savitribai Phule Pune University
Suresh Ghotekar (ghotekarsuresh7@gmail.com)
University of Mumbai, Dadra and Nagar Haveli https://orcid.org/0000-0001-7679-8344
Parita Basnet
Sikkim Manipal Universit
Van-Huy Nguyen
Binh Duong University
Shreyas Pansambal
Savitribai Phule Pune University
H C Ananda Murthy
Adama Science and Technology University
Thanh-Dong Pham
Vietnam National University
Muhammad Bilal
Huaiyin Institute of Technology
Rajeshwari Oza
Savitribai Phule Pune University
Vanita Karande
Yashavantrao Chavan Institute of Science

Research Article

Keywords: Green nanotechnology, Solanum elaeagnifolium, Ag-AgO-Ag2O NCs, Biomedical applications

Posted Date: October 21st, 2021

Abstract

The biogenic nanocomposite synthesis using a plant extract is rapid, simple, efficient, cost-effective, and eco-friendly. This study investigated selective pharmacological activities such as anticancer, antioxidant, and DNA cleavage activities of *Solanum elaeagnifolium*-mediated green synthesizing Ag-AgO-Ag_2O nanocomposite. To the best of our knowledge, *Solanum elaeagnifolium* has been the first time used to synthesize Ag-AgO-Ag_2O nanocomposites. The synthesized nanocomposites were explored by using UV-Vis diffuse reflectance spectroscopy, X-ray diffraction, Fourier transform infrared spectroscopy, scanning electron microscopy, high-resolution transmission electron microscopy, energy-dispersive X-ray spectroscopy, and photoluminescence analyses. Anticancer activity of Ag-AgO-Ag_2O nanocomposites was tested on lung cancer cell lines (A-549) and showed activity at the IC_{50} of 67.09 µg/mL. The maximum ABTS and DPPH scavenging activity were 25.78% and 20.86% at 100 µg/L, respectively. Moreover, *Solanum elaeagnifolium*-mediated green synthesized Ag-AgO-Ag_2O nanocomposites also exhibited considerable DNA cleavage activity. These results assured that the synthesized Ag-AgO-Ag_2O nanocomposites using *Solanum elaeagnifolium* leaves extract may have potential applications in biomedical engineering.

1. Introduction

Nowadays, nanotechnology has stupendous and enormous applications in many sectors of applied science and engineering like agriculture, biotechnology, dye degradation, food technology, wastewater treatment, energy, storage, ceramics, cosmetics, medical applications, drug delivery, bio-sensing, fabric, and textile engineering, etc. [1–4]. In particular, metal oxide nanoparticles (NPs) have attracted extensive attention.

Many types of NPs, such as Ag_2O [5], CaO [6], SnO_2 [7], Cr_2O_3 [8], CdO [9], CuO [10], Fe_3O_4 [11], MgO [12], Co_3O_4 [13], La_2O_3 [14], ZnO [15], and ZrO_2 [16], have been prepared and applied in various promising applications. They could be manufactured by biological, chemical, and physical approaches; nevertheless, biological protocols are the most recommended and sustainable approach since chemical, and physical approaches have numerous downsides [12, 17, 18]. Notably, the eco-friendly approach makes use of algae [19], bio-waste materials [20, 21], microorganisms [22], and plants [7, 8, 10]. Green synthesis using various medicinal plant parts is most rapid, simple, clean, easy, affordable, and environmentally gracious [23]. The varied plant parts contain a variety of structurally diverse natural biochemicals such as vitamins, alkaloids, anthocyanins, flavonoids, coumarins, phenols, sugars, glycosides, volatile oils, saponins, tannins, which themselves serve as bio-reducing and/or bio-stabilizing agents for nanoparticles production and hence obviating the use of noxious chemicals and solvents [24].

Among diverse nanoparticles, silver-based nanoparticles, such as Ag, AgCl, Ag_2O, and Ag_2S nanoparticles, are creating stupendous attention in the scientific arena due to their massive range of application in agriculture [25], biomedical devices [26], catalysis [27], ceramics [28], environmental remediation [5, 29],

pharmaceuticals [30], photocatalysis [5, 29, 31], and sensing [32]. The selective morphology and size of the silver-based nanoparticles is the deciding factor of their chemical and physical features [33]. Heretofore, various approaches, such as the hydrothermal method [34], microwave-assisted method [35, 36], sol-gel method [37], thermal decomposition [38], have been reported for the manufacturing of silver-based nanoparticles. Previously, facile biosynthesis of silver-based nanoparticles using plant extracts such as *Acanthospermum hispidum* [39], *Rosa sinensis* [40], *Leucaena leucocephala* [41], *Centella asiatica* [42], *Prunus persica* [43], and *Cochlospermum gossypium* [44] have been reported as a bio-reducing/bio-stabilizing agent, and their multifunctional applications are widely investigated.

Noticeably, *Solanum elaeagnifolium* of the family *Solanaceae*, is a deep-rooted perennial plant that is found initially native to the Americas. As summarized in Fig. 1, *Solanum elaeagnifolium* extract contains several bioactive compounds, namely stigmasterol, kaempferol, C-glycoside, quercetin, mangiferin, rutin, chlorogenic acid, coumaroyl glycoside, dicaffeoyl quinic acid [45–47]. Also, leaves from *Solanum elaeagnifolium* have repellent and insecticidal characteristics towards various crop pests and possibly be used as an alternative for synthetic insecticides [48]. To the best of our knowledge, *Solanum elaeagnifolium* has been examined for its pharmacological effects, but it has never been employed to synthesize Ag-AgO-Ag_2O nanocomposites.

Herein, this contribution reports on Ag-AgO-Ag_2O nanocomposites engineered by an entirely green chemistry approach using *Solanum elaeagnifolium* natural extract as a fuel addition of any chemical additives. To further characterize the material, Ag-AgO-Ag_2O nanocomposites were explored by various techniques. In addition, selective biomedical applications such as anticancer, antioxidant, and DNA cleavage activities were also investigated.

2. Experimental

2.1. Collection of Solanum elaeagnifolium leaves and extracts preparation

The *Solanum elaeagnifolium* leaves were collected and appropriately washed using double distilled water. 5g of leaves were poured into 100 mL of distilled water and boiled for 15 min at 85-90 ºC. The extract obtained was filtered through ordinary filter paper and then, Whatmann No. 1 filter paper. The filtered *Solanum elaeagnifolium* leaves extract (SELE) was stored at 4°C for Ag-AgO-Ag_2O NC synthesis.

2.2. Biosynthesis of Ag-AgO-Ag_2O nanocomposites

Eco-benign synthesis of Ag-AgO-Ag_2O nanocomposites involved adding 1.69 g silver nitrate to 100 mL of SELE, and then the reaction solution was stirred at 1100 rpm at room temperature with a magnetic stirrer. Initial confirmation of Ag-AgO-Ag_2O nanocomposites synthesis is by a change in color of the reaction mixture from yellow to dark brown. Then, the resulting solution was then centrifuged at room temperature

for 10 minutes at 3000 rpm. The black precipitates of material were dried at 200°C in a hot air oven. The obtained black color powder was stored in an airtight vial for further utilization.

2.3. Characterization of Ag-AgO-Ag_2O nanocomposites

Various characterization tools were used to examine the chemical, optical, and physical properties of Ag-AgO-Ag_2O nanocomposites. The XRD measurement of synthesized Ag-AgO-Ag_2O nanocomposites was carried out using a diffractometer system (XPERT-PRO, PANalytical). The UVDRS of Ag-AgO-Ag_2O nanocomposites were recorded using Jasco Spectrophotometer V-770. The functional groups analysis of biosynthesized Ag-AgO-Ag_2O nanocomposites was using FT-IR-4600typeA. The morphological features and elemental composition of bio-fabricated Ag-AgO-Ag_2O nanocomposites were studied by SEM equipped with EDX detector (VEGA3 TESCAN). Moreover, size and shape were studied using HRTEM (JEM-2100) operating at an accelerating 60-200 kV voltage. The photoluminescence nature of SELE-mediated Ag-AgO-Ag_2O nanocomposites was examined by using FP-8200 Spectroflurimeter.

2.4. Anticancer activity of Ag-AgO-Ag_2O nanocomposites

A549 lung cancer cells were procured from ATCC. Procured stock cells were grown in DMEM/RPMI supplemented with 10% inactivated Fetal Bovine Serum (FBS), penicillin (100 IU/ml), and streptomycin (100 µg/ml) in a humid environment of 5% CO_2 at 37 ºC. The cell was dissociated with cell dissociating solution (0.02 % EDTA, 0.2 % trypsin, and 0.05 % glucose in PBS). The vitality of the cells is tested, and the cells are centrifuged. In addition, 50,000 cells/well were seeded in a 96 well plate and incubated at 37 ºC under 5% CO_2 incubator for 24 hrs. Different concentrations of Ag-AgO-Ag_2O nanocomposites (10, 20, 40, 80, 160, and 320 µg/mL) was added and incubated at 37 ºC for 48 h [49]. The resulting solutions in the wells were removed after incubation, and 100 µl of MTT (5 mg/10 ml of MTT in PBS) was mixed with every well. The cultured plates were incubated at 37°C for 4 hours under 5% CO_2 environment. The supernatant was discarded, and 100 µl of DMSO was mixed into the plates, which were gently agitated to dissolve the formed formazan [50]. The viability of cell lines was measure at 570 nm by an ELISA reader. Triplicates of experiments were carried out, and Doxorubicin standard drug was used in the study as a positive control. The cell viability percentage was estimated by using the formula,

$$\%\mathrm{CellInhibition} = \frac{\mathrm{A_{570}oftest}}{\mathrm{A_{570}ofcontrol}} \times 100$$

2.5. In vitro antioxidant activity of Ag-AgO-Ag_2O nanocomposites

ABTS and DPPH radical scavenging assays were used to evaluate the in vitro antioxidant properties of the SELE-mediated Ag-AgO-Ag_2O nanocomposites. The varying concentrations of the Ag-AgO-Ag_2O nanocomposites and standard solution used were 20, 40, 60, 80, and 100 µg/mL. The study employed

ascorbic acid as a reference antioxidant. The absorbance was measured to the respective blank solutions using spectrophotometry [51, 52]. The following formula was used to compute the % inhibition:

$$\mathrm{Radicalscavengingactivity}(\%) = \frac{\mathrm{ODcontrol} - \mathrm{ODsample}}{\mathrm{ODcontrol}} \times 100$$

2.5.1. DPPH radical scavenging assay

Serial dilutions (20, 40, 60, 80, and 100 µg/mL) of Ag-AgO-Ag_2O nanocomposites were taken, and 50 µl of 0.659 mM 2,20-diphenyl-1-picrylhydrazyl (DPPH) dissolved in methanol was added, making up to one with distilled water. Thereafter, sample tubes were incubated for 20 minutes at 25°C [52]. A Shimadzu UV 1800 spectrophotometer was employed to record the absorbance at 510 nm.

2.5.2. ABTS radical scavenging assay

Serial dilutions (20, 40, 60, 80, and 100 µg/mL) of Ag-AgO-Ag_2O nanocomposites were taken, and 0.3 ml of ABTS radical cation [ABTS solution: 2, 20-Azino-bis(3-ethylbenzothiazoline-6-sulphonic acid) 2 mM (0.0548 gm in 50 ml)] was prepared in double-distilled water. Potassium per sulphate 70 mM was prepared in double-distilled water. After mixing 200 µl of potassium persulphate with 50 ml of ABTS for 2 hours, 1.7 ml of phosphate buffer pH 7.4 was mixed. After that, sample tubes were incubated for 20 minutes at 25 ºC [53]. A Shimadzu UV 1800 spectrophotometer was employed to record the absorbance at 734 nm.

2.6. DNA Cleavage activity of Ag-AgO-Ag_2O nanocomposites

The DNA cleavage activity of Ag-AgO-Ag_2O nanocomposites was studied using agarose gel electrophoresis. The plasmid DNA (pBR322) was employed as the target DNA for the cleavage activity. Different concentrations of pBR322 DNA molecules and Ag-AgO-Ag_2O nanocomposites were incubated for 30 and 90 min at 37 ºC. Thereafter, loading dye (0.25% bromphenol blue, 50% glycerol) was mixed into the reaction solution. The resulting mixtures were carried out on an electrophoresis gel using 0.8% agarose gel in TAE buffer (50 mM Tris base, 50 mM acetic acid, 2 mM EDTA, pH: 7.8) at 50 V [54]. Monitoring was done under UV light after the electrophoresis experiment.

3. Results And Discussion

3.1. Characterizations

The phase analysis, crystal structure, and composition of the SELE mediated Ag_xO sample was analyzed through the XRD technique, and the result is evinced in Fig. 2(a). It may be observed through this figure that three different phases are present in the sample corresponding to Ag (marked by *), AgO (marked by #), and Ag_2O (marked by ●). This indicates that the current method of biosynthesis led to the formation of

Ag-AgO-Ag_2O heterostructured nanocomposite. The existence of these phases was identified based on ICDD card no. 04-0783 [55], 84-1108 [56], and 42-0874 for metallic Ag, AgO, and Ag_2O, respectively [57–59]. This analysis, therefore, reveals that the three different phases are in the deposited form and not in the doped state since the diffraction peaks of all the phases are visible in the XRD spectrum.

Further, the unassigned peaks belong to $AgNO_3$, which was used as the Ag-precursor in this study [60]. This means that the operating temperature was insufficient to eradicate the salt precursor. Nevertheless, based on the intensity of the diffraction peaks, it may be noted that the most dominant phase in this sample is that of AgO. The average crystallite size of the sample was ascertained using the Scherrer equation and found to be 69.4 nm. Based on the XRD result, it is clear that the biosynthesized Ag_xO sample is composed of Ag-AgO-Ag_2O nanocomposites.

It notes that the plant phytochemicals perform two primary functions: (i) bio-reduction of the metal precursor and (ii) control over the particle size and shape. Herein, the functionalization of Ag-AgO-Ag_2O nanocomposites by these phytochemicals was confirmed from the FTIR studies. Fig. 2(b) represents the FTIR spectrum of the leaf extract of *Solanum elaeagnifolium* and Ag-AgO-Ag_2O nanocomposites. On comparing these FTIR spectra, it may be revealed that the bands at 1648.8 cm^{-1} and 1037.8 cm^{-1} of plant extract have wholly lost their intensities after functionalizing the nanocomposites. This means that during the biosynthesis procedure, the functional groups associated with the corresponding phytochemicals were mainly involved in the reducing mechanism of the salt precursor ($AgNO_3$) [61]. Contrariwise, the rest of the assigned bands have shifted their positions in the nanocomposites, which may be attributed to their anchoring onto the surface of the nanoparticles. The FTIR bands observed at 1743.9 cm^{-1} in plant extract and 1762.6 cm^{-1} in the nanocomposites correspond to the alkaloid functional group [62]. The band at 1643.8 cm^{-1} may be ascribed to the C=O stretching vibrations of the amide group majorly because of protein molecules present in the leaf extract [63]. The highly intense bands at ~1381 cm^{-1} may be attributed to the lipid functional group [64]. The band at 1037.8 cm^{-1} represents polysaccharides because of O-substituted glucose residue [65]. The band at 783.3 cm^{-1} is due to the C-H out-of-plane bend of phenyl [65]. This band has shifted to 825.1 cm^{-1} in the nanocomposites. Thus, based on the relative intensities of the prominent FTIR bands of plant extract and the as-synthesized Ag-AgO-Ag_2O nanocomposites, it may be concluded that protein and glucose metabolites were responsible for functioning as reductants, lipids, and alkaloid functional groups mainly exhibited the capping agent property. This means the latter functional groups have a more vital ability to bind with the Ag ions, and prevent their particles from the undesirable agglomeration phenomenon, thus, confirming the plant phytochemical screening test.

A typical SEM analysis was performed to study the morphological characteristic of the as-synthesized Ag-AgO-Ag_2O nanocomposites, as shown in Fig. 2(c). In contrast, EDX analysis was employed to detect the elemental composition of this sample, and the results are depicted in Fig. 2(d). The SEM image (Fig. 2(c)) revealed a high density of nanoparticles. Although the particles have mostly agglomerated, it is

n the individual particle grains. From this image,

the morphology of the particles was observed to be quasi-spherical in shape. The EDX analysis of Ag-AgO-Ag_2O nanocomposites (Fig. 2(d)) represents the existence of only Ag and O in the sample with no impurity peaks, indicating the method of biosynthesis employed in this study leads to the formation of impurity-free Ag-AgO-Ag_2O nanocomposites. The EDX analysis evinced percentage relative elemental composition, such as Ag (17.76%) and O (82.24%), as presented in the inset table of Fig. 2(d).

The microstructural analysis and particle size determination of the as-synthesized sample were performed through HRTEM studies, and the results have been shown in Fig. 3. It may be observed from the TEM images in Fig. 3(a-b) that the particles have formed quasi-spherical microstructure, which is consistent with the morphology obtained through SEM analysis. However, the particles did not exhibit monodispersity, and hence, their average diameter was calculated to be in the range of 15 nm to 40 nm. From Fig. 3(c), which represents the HRTEM image of Ag-AgO-Ag_2O nanocomposites, the appearance of criss-cross patterns is visible, further confirming the existence of different phases in this sample.

The optical absorbance of the as-synthesized sample was analyzed based on the UV-Vis absorbance data, and the corresponding spectra are presented in Fig. 4(a). This figure depicts the existence of two major absorbance bands at 295 nm and 455 nm. The band at 295 nm is due to the presence of the AgO component in the sample [55]. This means that AgO primarily absorbs in the UV-range. The broad absorbance maximum at 455 nm, as shown in Fig. 4(b), may be attributed to the absorbance contribution from the Ag and Ag_2O [5, 66] components present in the sample. As a result, the surface plasmon resonance (SPR) effect of Ag nanoparticles [55]. Generally, SPR for Ag nanoparticles is observed around 440 nm [65]. In this case, a shift in the SPR band may be attributed to the strong interfacial coupling of the Ag nanoparticles with the silver oxide components. Fig. 4(c) represents the Tauc plot fitted using the Tauc equation [67] for obtaining the bandgap energy of the as-synthesized sample, which was calculated to be 3.3 eV. Fig. 4(d) corresponds to the PL spectra of the as-synthesized sample. A single emission band centered at 576 nm was observed. This photoluminescence peak corresponds to the bandgap of the as-synthesized nanocomposites as well as its exciting state transition [68].

3.2. Anticancer activity

The anticancer efficacy of SELE mediated Ag-AgO-Ag_2O nanocomposites on human lung cancer cell line (A549) was investigated by MTT assay. For the anticancer study of SELE mediated Ag-AgO-Ag_2O nanocomposites on human lung cancer cell line, diverse concentrations of 10, 20, 40, 60, 80, and 100 µg mL^{-1} were employed, as displayed in Fig. 5. The biogenically fabricated Ag-AgO-Ag_2O nanocomposites have shown a significant cytotoxicity impact on a human lung cancer cell line, with IC_{50} value of 67.09 µg mL^{-1}, while Doxorubicin shows IC_{50} value of 20.66 µg mL^{-1} (Fig. 6). When the concentration of Ag-AgO-

Ag_2O nanocomposites was gradually increased to 360 μg mL^{-1} on a human lung cancer cell line, the percentage of cell viability was reduced to 18.28 %.

3.3. Antioxidant activity

The scavenging ability of the Ag-AgO-Ag_2O nanocomposites was evaluated using ABTS and DPPH scavenging assays. The radical scavenging potential of Ag-AgO-Ag2O nanocomposites was dependent on the concentration, increasing from 20 to 100 g μg mL^{-1} as the concentration of Ag-AgO-Ag2O nanocomposites (Fig. 7-ABTS and Fig. 8-DPPH). Ag-AgO-Ag_2O nanocomposites also showed ABTS radical scavenging performance with a maximal inhibition of 25.78%. The IC_{50} value of Ag-AgO-Ag_2O nanocomposites against ABTS radicals was 85.12 μg mL^{-1}. Ag-AgO-Ag_2O nanocomposites evinced a maximum scavenging inhibition of 20.86% against DPPH radicals with an IC_{50} value of 89.55 μg mL^{-1}. The antioxidant activity of Ag-AgO-Ag_2O nanocomposites justifies their usefulness in the pharmaceutical and biomedical sectors.

3.4. DNA cleavage activity

The gel electrophoresis was applied to investigate the DNA cleavage activity. Because of its optimal DNA cleavage ability, the biosynthesized Ag-AgO-Ag_2O nanocomposites have a good cleavage performance than the control. Ag-AgO-Ag_2O nanocomposites acted on plasmid DNA molecules, as shown by electrophoresis. The DNA cleavage activity of as-synthesized Ag-AgO-Ag_2O nanocomposites is displayed in Fig. 9. When compared to control DNA, there are changes in the bands of Lanes 2-5, as indicated in Fig. 9. In Lanes 2-4, the plasmid pBR322 was altered from Form I to Form II. Furthermore, the observations revealed that the SELE-mediated Ag-AgO-Ag_2O nanocomposites behaved as chemical nucleases by cleaving DNA Form I into Form III at a concentration of 1 μl for 90 min. This study demonstrated that Ag-AgO-Ag_2O nanocomposites could be employed as an alternative cancer therapy as a DNA target drug.

4. Conclusion

The green chemistry approach was used for the production of Ag-AgO-Ag_2O nanocomposites, and SELE was chosen as a natural reducing and/or stabilizing agent in our experiment. It was revealed that the SELE could be successfully employed for the facile synthesis of Ag-AgO-Ag_2O nanocomposites at room temperature. SELE mediated green synthesizing Ag-AgO-Ag_2O nanocomposites were explored using UVDRS, XRD, FTIR, SEM, HRTEM, EDX and PL analysis. In the HRTEM analysis of Ag-AgO-Ag_2O nanocomposites, quasi-spherical shaped particles were obtained. The mean diameter of the Ag-AgO-Ag_2O nanocomposites was found to be 69.4 nm. It was observed that synthesized Ag-AgO-Ag_2O

nanocomposites showed sound anticancer effects against A-549 lung cancer cell lines. However, antioxidant and DNA cleavage results have also been shown to be effective for Ag-AgO-Ag_2O nanocomposites. The current study has revealed the possibility of executing SELE-mediated Ag-AgO-Ag_2O nanocomposites, which might be exploited as an antioxidant, DNA cleavage, and anticancer agent.

Declarations

Conflict of interest

The authors declare that there are no conflicts of interest regarding the publication of this manuscript.

References

[1] W. Lin, Introduction: nanoparticles in medicine, Chemical reviews, 115 (2015) 10407-10409.

[2] N.T. Thanh, N. Maclean, S. Mahiddine, Mechanisms of nucleation and growth of nanoparticles in solution, Chemical reviews, 114 (2014) 7610-7630.

[3] B. Devadas, A.P. Periasamy, K. Bouzek, A review on poly (amidoamine) dendrimer encapsulated nanoparticles synthesis and usage in energy conversion and storage applications, Coordination Chemistry Reviews, 444 (2021) 214062.

[4] M.B. Gawande, A. Goswami, F.-X. Felpin, T. Asefa, X. Huang, R. Silva, X. Zou, R. Zboril, R.S. Varma, Cu and Cu-based nanoparticles: synthesis and applications in catalysis, Chemical reviews, 116 (2016) 3722-3811.

[5] S. Ghotekar, H. Dabhane, S. Pansambal, R. Oza, P. Tambade, V. Medhane, A review on biomimetic synthesis of Ag2O nanoparticles using plant extract, characterization and its recent applications, Advanced Journal of Chemistry-Section B, 2 (2020) 102-111.

[6] T. Pagar, S. Ghotekar, S. Pansambal, R. Oza, B.P. Marasini, Facile plant extract mediated eco-benevolent synthesis and recent applications of CaO-NPs: A state-of-the-art review, Journal of Chemical Reviews, 2 (2020) 201-210.

[7] S. Matussin, M.H. Harunsani, A.L. Tan, M.M. Khan, Plant-extract-mediated SnO2 nanoparticles: synthesis and applications, ACS Sustainable Chemistry & Engineering, 8 (2020) 3040-3054.

[8] S. Ghotekar, S. Pansambal, M. Bilal, S.S. Pingale, R. Oza, Environmentally friendly synthesis of Cr2O3 nanoparticles: Characterization, applications and future perspective– a review, Case Studies in Chemical and Environmental Engineering, 3 (2021) 100089.

[9] S. Ghotekar, A review on plant extract mediated biogenic synthesis of CdO nanoparticles and their recent applications, Asian Journal of Green Chemistry, 3 (2019) 187-200.

[10] H.N. Cuong, S. Pansambal, S. Ghotekar, R. Oza, N.T.T. Hai, N.M. Viet, V.-H. Nguyen, New frontiers in the plant extract mediated biosynthesis of copper oxide (CuO) nanoparticles and their potential applications: A review, Environmental Research, (2021) 111858.

[11] Y.P. Yew, K. Shameli, M. Miyake, N.B.B.A. Khairudin, S.E.B. Mohamad, T. Naiki, K.X. Lee, Green biosynthesis of superparamagnetic magnetite Fe3O4 nanoparticles and biomedical applications in targeted anticancer drug delivery system: A review, Arabian Journal of Chemistry, 13 (2020) 2287-2308.

[12] H. Dabhane, S. Ghotekar, P. Tambade, S. Pansambal, H.A. Murthy, R. Oza, V. Medhane, A review on environmentally benevolent synthesis of CdS nanoparticle and their applications, Environmental Chemistry and Ecotoxicology, (2021).

[13] T. Pagar, S. Ghotekar, K. Pagar, S. Pansambal, R. Oza, A Review on Bio-Synthesized Co3O4 Nanoparticles Using Plant Extracts and their Diverse Applications, Journal of Chemical Reviews, 1 (2019) 260-270.

[14] H. Dabhane, S. Ghotekar, P. Tambade, V. Medhane, Plant mediated green synthesis of lanthanum oxide (La2O3) nanoparticles: A review, Asian Journal of Nanosciences and Materials, 3 (2020) 291-299.

[15] M. Bandeira, M. Giovanela, M. Roesch-Ely, D.M. Devine, J. da Silva Crespo, Green synthesis of zinc oxide nanoparticles: A review of the synthesis methodology and mechanism of formation, Sustainable Chemistry and Pharmacy, 15 (2020) 100223.

[16] A. Nikam, T. Pagar, S. Ghotekar, K. Pagar, S. Pansambal, A review on plant extract mediated green synthesis of zirconia nanoparticles and their miscellaneous applications, Journal of chemical reviews, 1 (2019) 154-163.

[17] P. Korde, S. Ghotekar, T. Pagar, S. Pansambal, R. Oza, D. Mane, Plant extract assisted eco-benevolent synthesis of selenium nanoparticles-a review on plant parts involved, characterization and their recent applications, Journal of Chemical Reviews, 2 (2020) 157-168.

[18] A.C. Paiva-Santos, A.M. Herdade, C. Guerra, D. Peixoto, M. Pereira-Silva, M. Zeinali, F. Mascarenhas-Melo, A. Paranhos, F. Veiga, Plant-mediated green synthesis of metal-based nanoparticles for dermopharmaceutical and cosmetic applications, International Journal of Pharmaceutics, (2021) 120311.

[19] S. AlNadhari, N.M. Al-Enazi, F. Alshehrei, F. Ameen, A review on biogenic synthesis of metal nanoparticles using marine algae and its applications, Environmental Research, 194 (2021) 110672.

[20] A. Santhosh, V. Theertha, P. Prakash, S.S. Chandran, From waste to a value added product: Green synthesis of silver nanoparticles from onion peels together with its diverse applications, Materials Today: Proceedings, 46 (2021) 4460-4463.

[21] H. Dabhane, S.K. Ghotekar, P.J. Tambade, S. Pansambal, H. Ananda Murthy, R. Oza, V. Medhane, Cow Urine Mediated Green Synthesis of Nanomaterial and Their Applications: A State-of-the-art Review, Journal of Water and Environmental Nanotechnology, 6 (2021) 81-91.

[22] S. Ibrahim, Z. Ahmad, M.Z. Manzoor, M. Mujahid, Z. Faheem, A. Adnan, Optimization for biogenic microbial synthesis of silver nanoparticles through response surface methodology, characterization, their antimicrobial, antioxidant, and catalytic potential, Scientific Reports, 11 (2021) 1-18.

[23] V. Soni, P. Raizada, P. Singh, H.N. Cuong, S. Rangabhashiyam, A. Saini, R.V. Saini, Q. Van Le, A.K. Nadda, T.-T. Le, Sustainable and green trends in using plant extracts for the synthesis of biogenic metal nanoparticles toward environmental and pharmaceutical advances: A review, Environmental Research, (2021) 111622.

[24] M. Nasrollahzadeh, M. Sajjadi, J. Dadashi, H. Ghafuri, Pd-based nanoparticles: Plant-assisted biosynthesis, characterization, mechanism, stability, catalytic and antimicrobial activities, Advances in colloid and interface science, 276 (2020) 102103.

[25] A.M. Partila, Bioproduction of silver nanoparticles and its potential applications in agriculture, in: Nanotechnology for Agriculture, Springer, 2019, pp. 19-36.

[26] S.P. Singh, C. Bhargava, V. Dubey, A. Mishra, Y. Singh, Silver nanoparticles: Biomedical applications, toxicity, and safety issues, International Journal of Research in Pharmacy and Pharmaceutical Sciences, 4 (2017) 01-10.

[27] M. A Bhosale, B. M Bhanage, Silver nanoparticles: Synthesis, characterization and their application as a sustainable catalyst for organic transformations, Current Organic Chemistry, 19 (2015) 708-727.

[28] F. Göl, A. Aygün, A. Seyrankaya, T. Gür, C. Yenikaya, F. Şen, Green synthesis and characterization of Camellia sinensis mediated silver nanoparticles for antibacterial ceramic applications, Materials Chemistry and Physics, 250 (2020) 123037.

[29] S. Ghotekar, K. Pagar, S. Pansambal, H.A. Murthy, R. Oza, Biosynthesis of silver sulfide nanoparticle and its applications, in: Handbook of Greener Synthesis of Nanomaterials and Compounds, Elsevier, 2021, pp. 191-200.

[30] N. Durán, G. Nakazato, A.B. Seabra, Antimicrobial activity of biogenic silver nanoparticles, and silver chloride nanoparticles: an overview and comments, Applied microbiology and biotechnology, 100 (2016) 6555-6570.

[31] S. Marimuthu, A.J. Antonisamy, S. Malayandi, K. Rajendran, P.-C. Tsai, A. Pugazhendhi, V.K. Ponnusamy, Silver nanoparticles in dye effluent treatment: A review on synthesis, treatment methods, mechanisms, photocatalytic degradation, toxic effects and mitigation of toxicity, Journal of Photochemistry and Photobiology B: Biology, 205 (2020) 111823.

[32] C.K. Tagad, S.R. Dugasani, R. Aiyer, S. Park, A. Kulkarni, S. Sabharwal, Green synthesis of silver nanoparticles and their application for the development of optical fiber based hydrogen peroxide sensor, Sensors and Actuators B: Chemical, 183 (2013) 144-149.

[33] R.K. Sharma, S. Yadav, S. Dutta, H.B. Kale, I.R. Warkad, R. Zbořil, R.S. Varma, M.B. Gawande, Silver nanomaterials: synthesis and (electro/photo) catalytic applications, Chemical Society Reviews, (2021).

[34] J. Yang, J. Pan, Hydrothermal synthesis of silver nanoparticles by sodium alginate and their applications in surface-enhanced Raman scattering and catalysis, Acta Materialia, 60 (2012) 4753-4758.

[35] B.M. Al-Shehri, M. Shkir, T.M. Bawazeer, S. AlFaify, M.S. Hamdy, A rapid microwave synthesis of Ag2S nanoparticles and their photocatalytic performance under UV and visible light illumination for water treatment applications, Physica E: Low-dimensional Systems and Nanostructures, 121 (2020) 114060.

[36] P.J. Babu, M. Doble, A.M. Raichur, Silver oxide nanoparticles embedded silk fibroin spuns: Microwave mediated preparation, characterization and their synergistic wound healing and anti-bacterial activity, Journal of colloid and interface science, 513 (2018) 62-71.

[37] M. Shahjahan, H. Rahman, M.S. Hossain, M.A. Khatun, A. Islam, M.H.A. Begum, Synthesis and characterization of silver nanoparticles by sol-gel technique, Nanosci. Nanometrol, 3 (2017) 34-39.

[38] S.M. Hosseinpour-Mashkani, M. Ramezani, Silver and silver oxide nanoparticles: Synthesis and characterization by thermal decomposition, Materials Letters, 130 (2014) 259-262.

[39] S. Ghotekar, S. Pansambal, S.P. Pawar, T. Pagar, R. Oza, S. Bangale, Biological activities of biogenically synthesized fluorescent silver nanoparticles using Acanthospermum hispidum leaves extract, SN Applied Sciences, 1 (2019) 1-12.

[40] S. Bangale, S. Ghotekar, Bio-fabrication of Silver nanoparticles using Rosa Chinensis L. extract for antibacterial activities, International Journal of Nano Dimension, 10 (2019) 217-224.

[41] S. Ghotekar, A. Savale, S. Pansambal, Phytofabrication of fluorescent silver nanoparticles from Leucaena leucocephala L. leaves and their biological activities, Journal of Water and Environmental Nanotechnology, 3 (2018) 95-105.

[42] B. Rashmi, S.F. Harlapur, B. Avinash, C. Ravikumar, H. Nagaswarupa, M.A. Kumar, K. Gurushantha, M. Santosh, Facile green synthesis of silver oxide nanoparticles and their electrochemical, photocatalytic and biological studies, Inorganic Chemistry Communications, 111 (2020) 107580.

[43] J.K. Patra, K.-H. Baek, Green synthesis of silver chloride nanoparticles using Prunus persica L. outer peel extract and investigation of antibacterial, anticandidal, antioxidant potential, Green Chemistry Letters and Reviews, 9 (2016) 132-142.

[44] D. Ayodhya, G. Veerabhadram, Green synthesis, characterization, photocatalytic, fluorescence and antimicrobial activities of Cochlospermum gossypium capped Ag2S nanoparticles, Journal of Photochemistry and Photobiology B: Biology, 157 (2016) 57-69.

[45] A. Badawy, R. Zayed, S. Ahmed, H. Hassanean, Phytochemical and pharmacological studies of Solanum elaeagnifolium growing in Egypt, Journal of Natural Products, 6 (2013) 156-167.

[46] F.A. Elabbar, N.M. Bozkeha, A.T. El-Tuonsia, Extraction, separation and identification of compounds from leaves of Solanum elaeagnifolium Cav.(Solanaceae), International Current Pharmaceutical Journal, 3 (2014) 234-239.

[47] M.A. Balah, G.M. AbdelRazek, Pesticidal activity of Solanum elaeagnifolium Cav. Leaves against nematodes and perennial weeds, Acta Ecologica Sinica, 40 (2020) 373-379.

[48] A.B. Hamouda, K. Zarrad, A. Laarif, I. Chaieb, Insecticidal effect of Solanum elaeagnifolium extracts under laboratory conditions, Journal of Entomology and Zoology Studies, 3 (2015) 187-190.

[49] R. Gonzalez, J. Tarloff, Evaluation of hepatic subcellular fractions for Alamar blue and MTT reductase activity, Toxicology in vitro, 15 (2001) 257-259.

[50] T. Sangeethaa, S. Mohanapriyab, N. Bhuvaneswaric, Synthesis, characterization and biological evaluation of heterocyclic triazole derived Schiff base ligands comprising Mn (II) complexes: Implications of their DNA/protein binding docking and anticancer activity studies, (2021).

[51] D. Rehana, D. Mahendiran, R.S. Kumar, A.K. Rahiman, Evaluation of antioxidant and anticancer activity of copper oxide nanoparticles synthesized using medicinally important plant extracts, Biomedicine & Pharmacotherapy, 89 (2017) 1067-1077.

[52] P. Jain, R. Agrawal, Antioxidant and free radical scavenging properties of developed mono-and polyherbal formulations, Asian J. Exp. Sci, 22 (2008) 213-220.

[53] N. Jamila, N. Khan, N. Bibi, M. Waqas, S.N. Khan, A. Atlas, F. Amin, F. Khan, M. Saba, Hg (II) sensing, catalytic, antioxidant, antimicrobial, and anticancer potential of Garcinia mangostana and α-mangostin mediated silver nanoparticles, Chemosphere, 272 (2021) 129794.

[54] F. Gulbagca, A. Aygün, M. Gülcan, S. Ozdemir, S. Gonca, F. Şen, Green synthesis of palladium nanoparticles: Preparation, characterization, and investigation of antioxidant, antimicrobial, anticancer, and DNA cleavage activities, Applied Organometallic Chemistry, (2021) e6272.

[55] B. Gauri, K. Vidya, D. Sharada, W. Shobha, Synthesis and characterization of Ag/AgO nanoparticles as alcohol sensor, Res J Chem Environ, 20 (2016) 1-5.

[56] T. Varthini, G. Carmel Vijila, M. Jothi, Effect of Medicinal Leaf Extract In Silver Nitrate-Size Reduction

[57] A. Ziashahabi, M. Prato, Z. Dang, R. Poursalehi, N. Naseri, The effect of silver oxidation on the photocatalytic activity of Ag/ZnO hybrid plasmonic/metal-oxide nanostructures under visible light and in the dark, Scientific reports, 9 (2019) 1-12.

[58] H. Yang, Y.-y. Ren, T. Wang, C. Wang, Preparation and antibacterial activities of Ag/Ag+/Ag3+ nanoparticle composites made by pomegranate (Punica granatum) rind extract, Results in physics, 6 (2016) 299-304.

[59] G.I. Waterhouse, G.A. Bowmaker, J.B. Metson, The thermal decomposition of silver (I, III) oxide: A combined XRD, FT-IR and Raman spectroscopic study, Physical Chemistry Chemical Physics, 3 (2001) 3838-3845.

[60] S.B. Aziz, R.T. Abdulwahid, M.A. Rasheed, O.G. Abdullah, H.M. Ahmed, Polymer blending as a novel approach for tuning the SPR peaks of silver nanoparticles, Polymers, 9 (2017) 486.

[61] P. Basnet, T.I. Chanu, D. Samanta, S. Chatterjee, A review on bio-synthesized zinc oxide nanoparticles using plant extracts as reductants and stabilizing agents, Journal of Photochemistry and Photobiology B: Biology, 183 (2018) 201-221.

[62] I. Masterova, J. Tomko, Isolation and identification of alkaloids from Frítillaria imperíalis L. var. rubra maxima, Chem. zvesti, 32 (1978) 116-119.

[63] T. Durak, J. Depciuch, Effect of plant sample preparation and measuring methods on ATR-FTIR spectra results, Environmental and Experimental Botany, 169 (2020) 103915.

[64] K. Velsankar, S. Sudhahar, G. Parvathy, R. Kaliammal, Effect of cytotoxicity and aAntibacterial activity of biosynthesis of ZnO hexagonal shaped nanoparticles by Echinochloa frumentacea grains extract as a reducing agent, Materials Chemistry and Physics, 239 (2020) 121976.

[65] P. Basnet, D. Samanta, T.I. Chanu, J. Mukherjee, S. Chatterjee, Tea-phytochemicals functionalized Ag modified ZnO nanocomposites for visible light driven photocatalytic removal of organic water pollutants, Materials Research Express, 6 (2019) 085095.

[66] W.M. Shume, H. Murthy, E.A. Zereffa, A review on synthesis and characterization of Ag2O nanoparticles for photocatalytic applications, Journal of Chemistry, 2020 (2020).

[67] A. Dolgonos, T.O. Mason, K.R. Poeppelmeier, Direct optical band gap measurement in polycrystalline semiconductors: A critical look at the Tauc method, Journal of solid state chemistry, 240 (2016) 43-48.

[68] T.-H. Lin, T.-T. Chen, C.-L. Cheng, H.-Y. Lin, Y.-F. Chen, Selectively enhanced band gap emission in ZnO/Ag 2 O nanocomposites, Optics express, 17 (2009) 4342-4347.

Figures

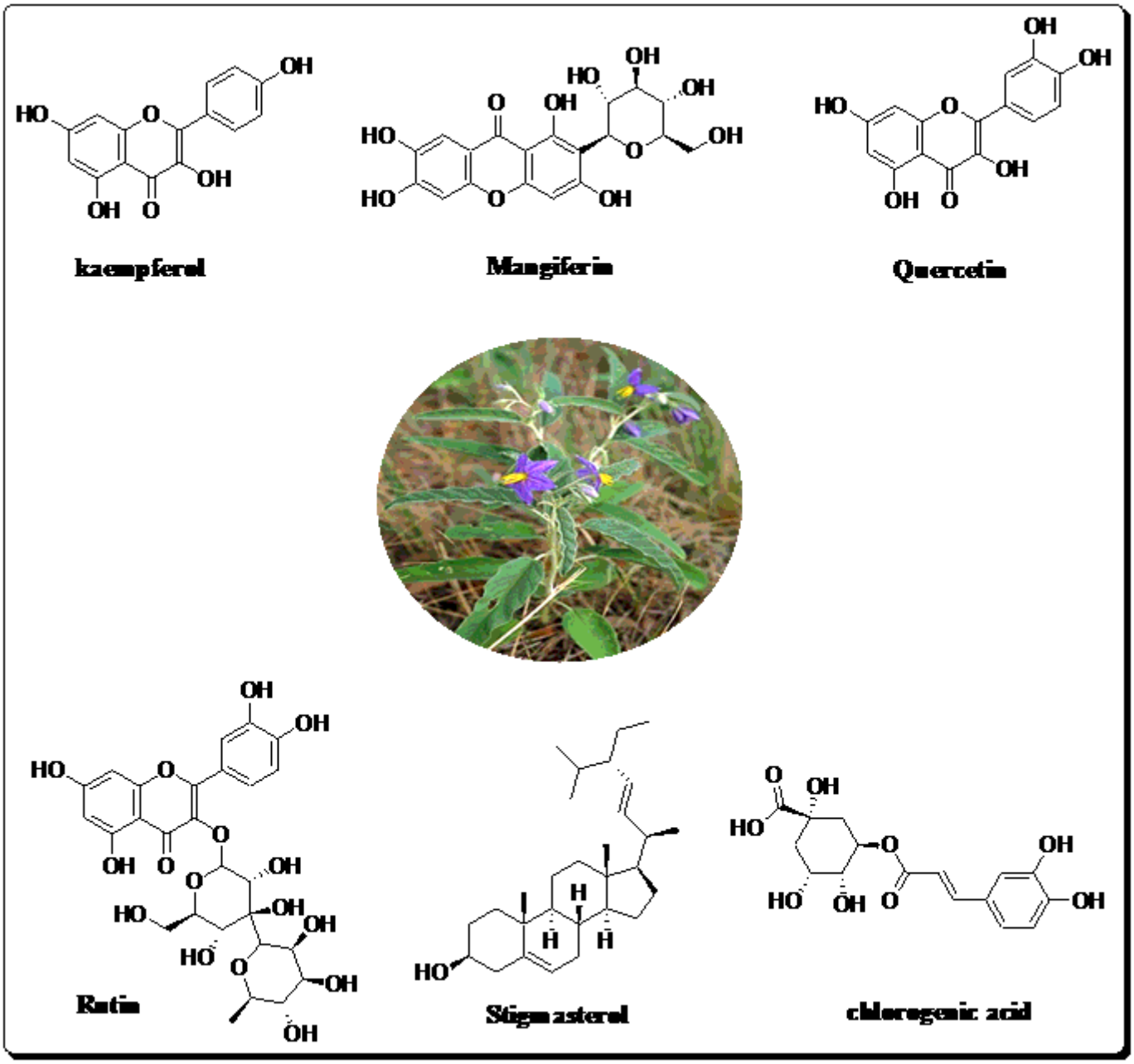

Figure 1

Active phytochemical in Solanum elaeagnifolium

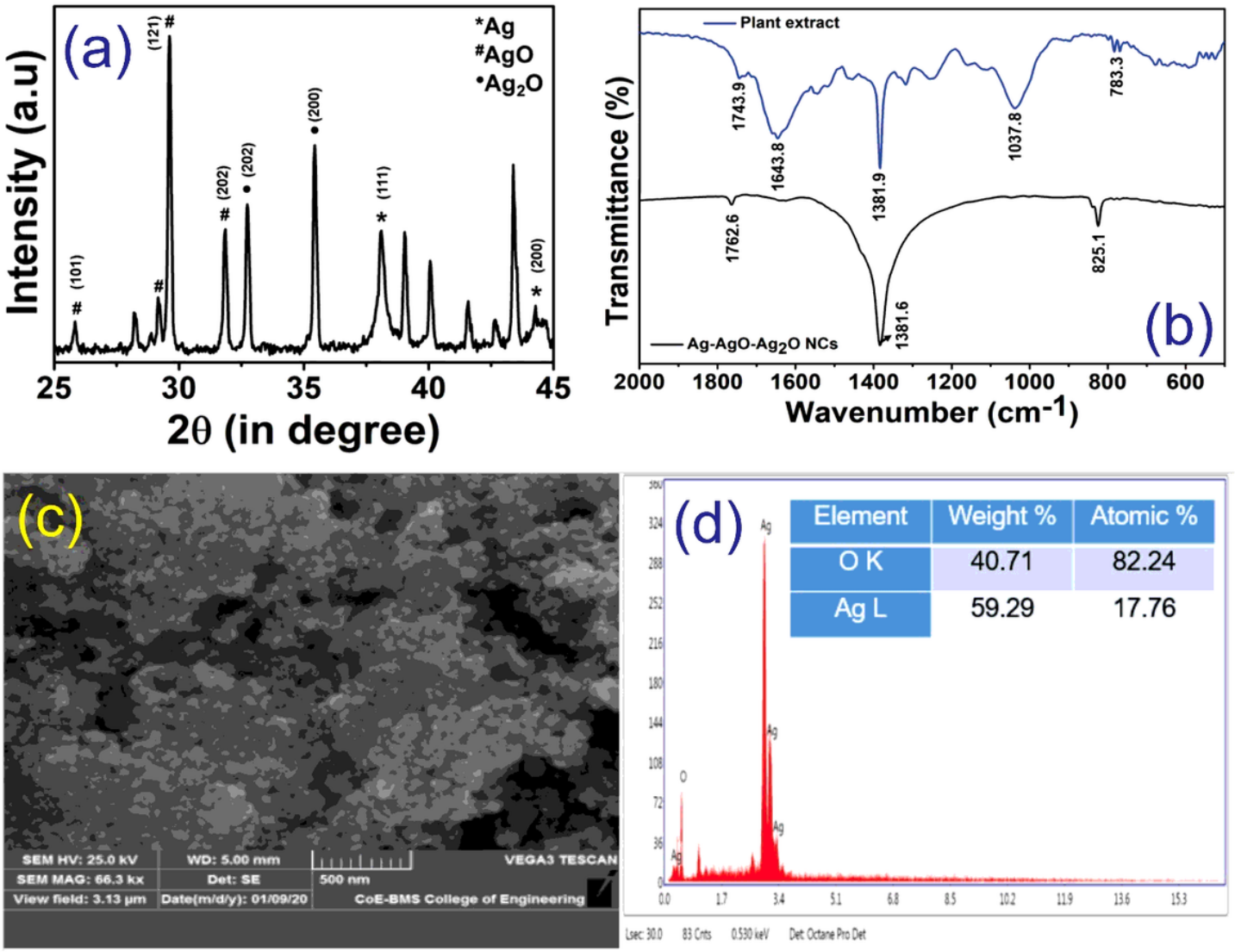

Figure 2

Characterizations of Ag-AgO-Ag2O nanocomposites: (a) XRD, (b) FTIR spectra of Solanum elaeagnifolium leaf extract (plant extract), and Ag-AgO-Ag2O nanocomposites, (c) SEM image, and (b) EDX spectra

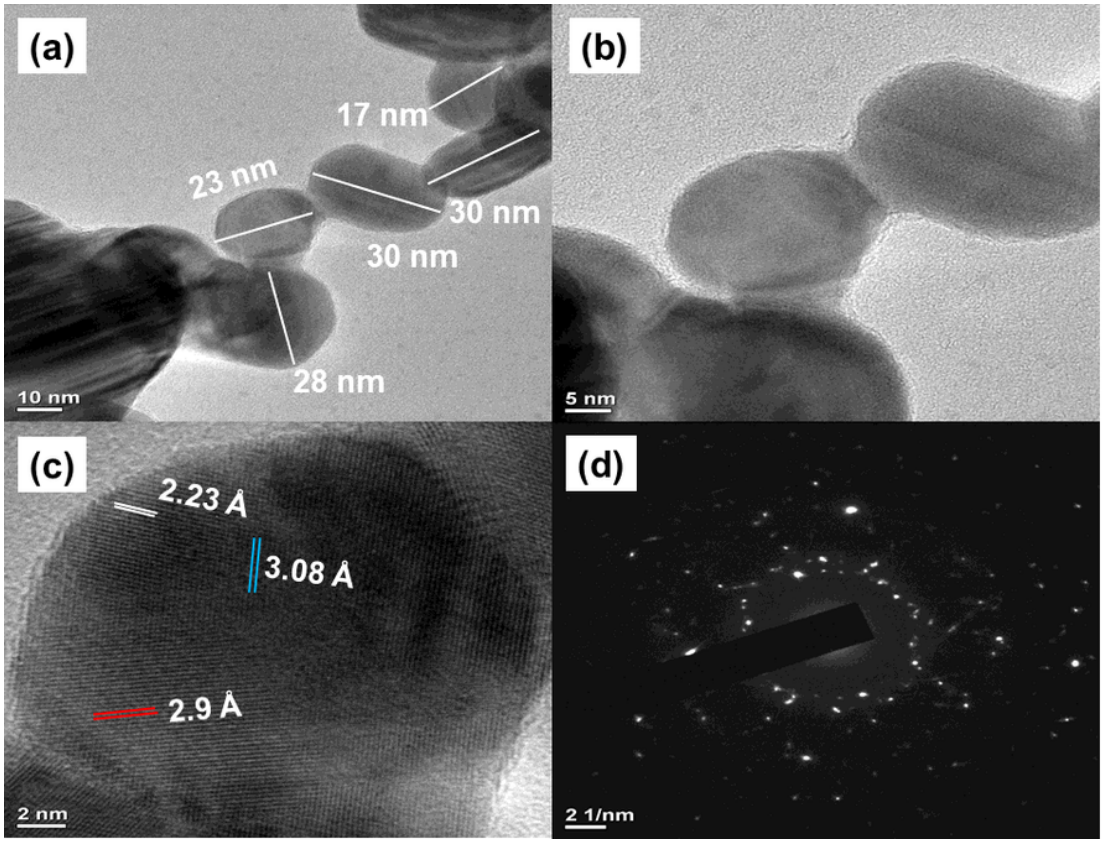

Figure 3

(a-b) TEM image, (c) HRTEM image displaying the lattice fringes, and (d) SAED pattern of Ag-AgO-Ag2O nanocomposites

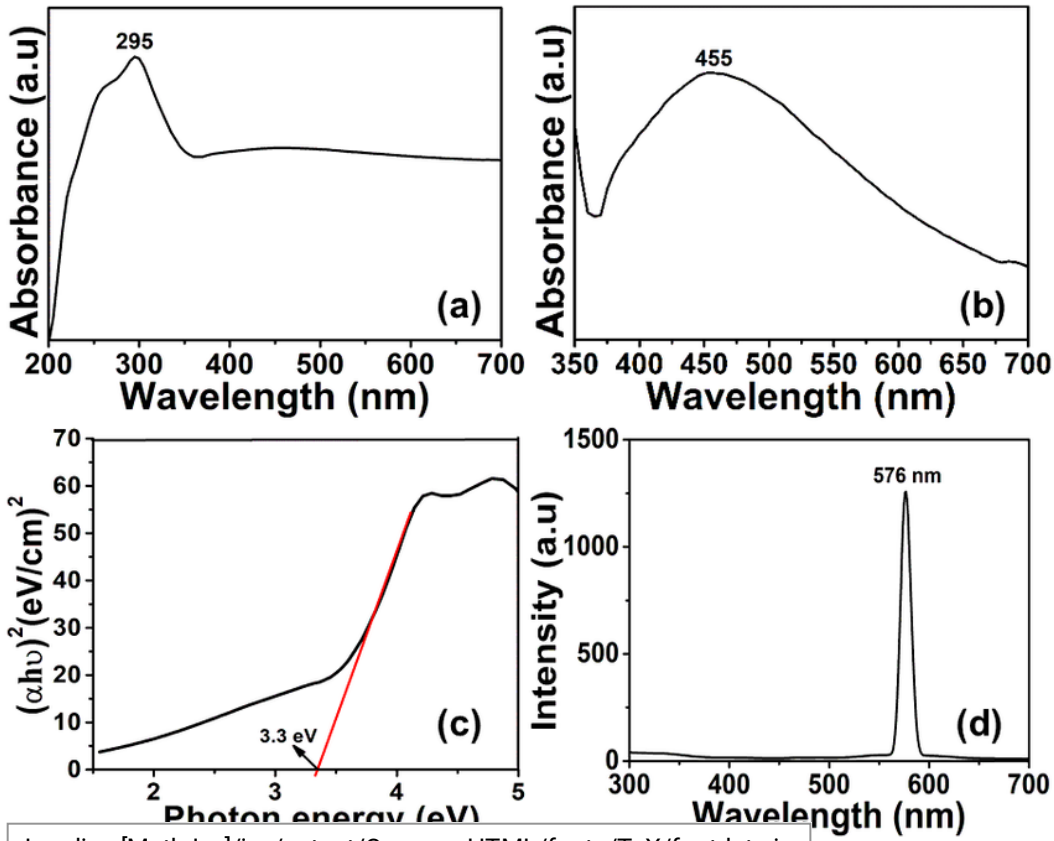

Figure 4

(a) UV-Vis absorbance spectra of Ag-AgO-Ag2O nanocomposites, (b) Magnified UV-Vis absorbance spectra ranging from 350 to 700 nm, (c) Tauc-plot for optical band gap energy determination, and (d) PL spectra

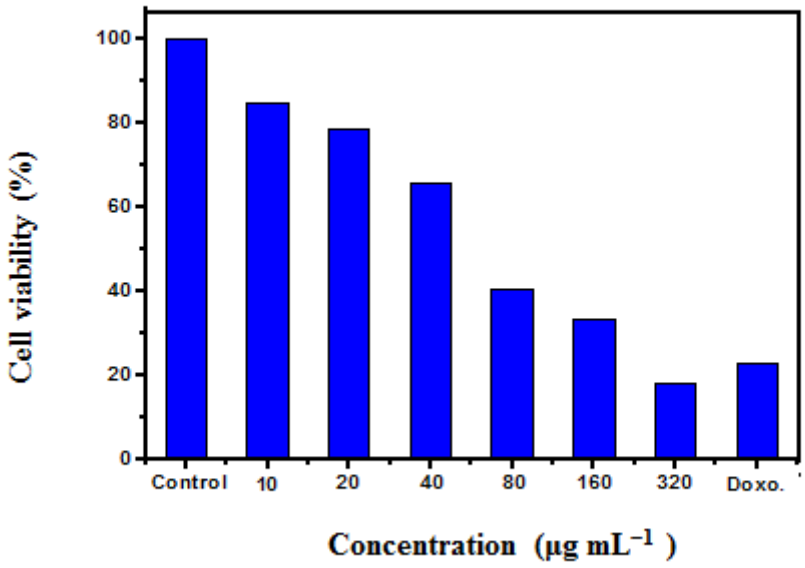

Figure 5

Anticancer activity of bio-inspired synthesis of Ag-AgO-Ag2O nanocomposites from SELE

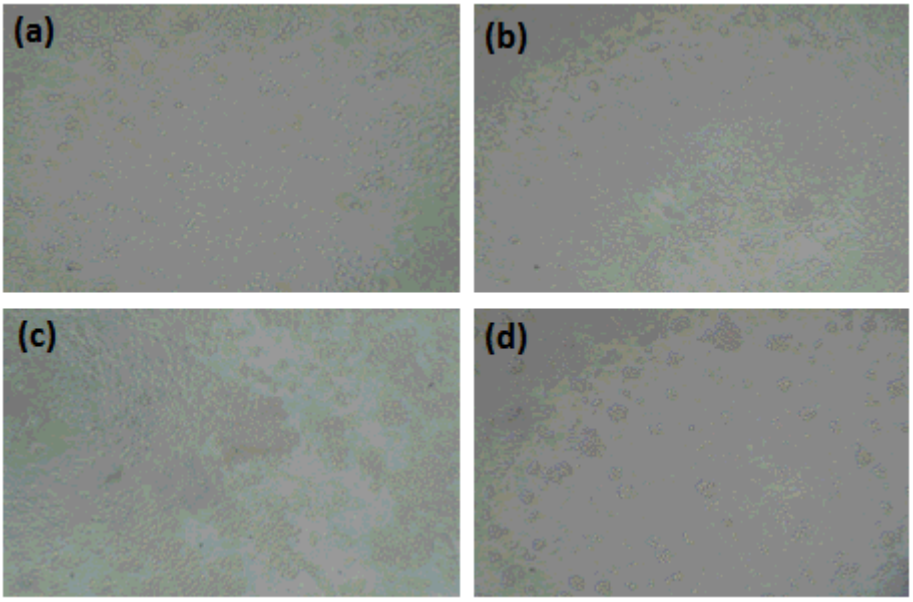

Figure 6

Anticancer activity of SELE mediated Ag-AgO-Ag2O nanocomposites, (a) control (b) 10 µg mL−1 (c) 360 µg mL−1 (d) doxorubicin 100 µg mL−1

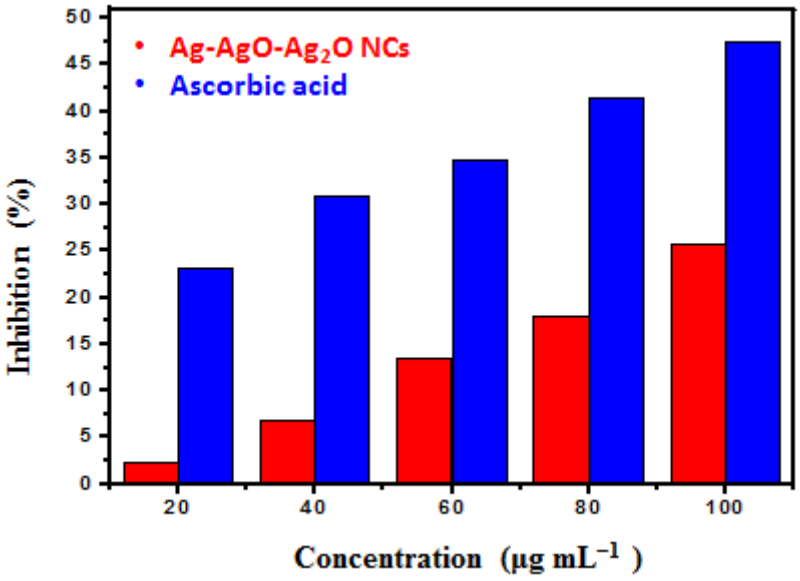

Figure 7

Antioxidant activities of Ag-AgO-Ag2O nanocomposites and ascorbic acid using ABTS assay

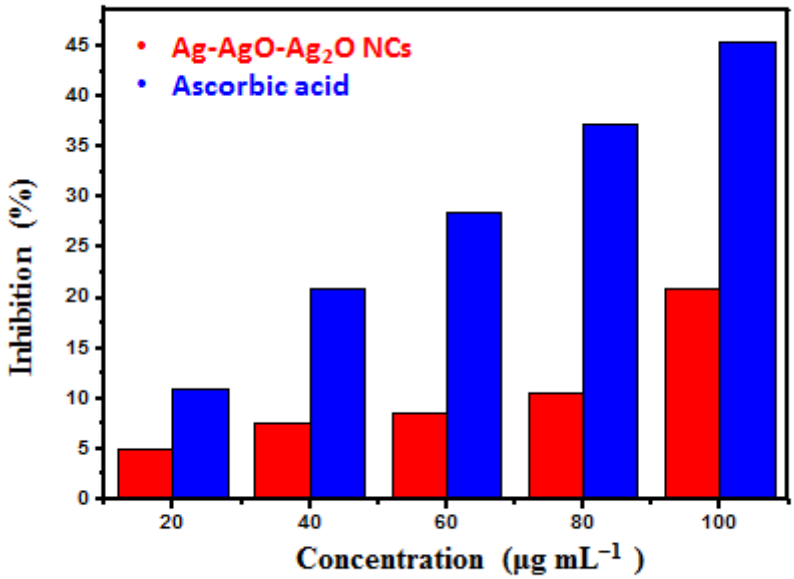

Figure 8

Antioxidant activities of Ag-AgO-Ag2O nanocomposites and ascorbic acid using DPPH assay

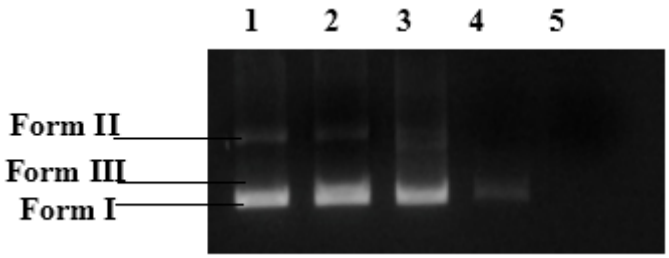

Figure 9

Lane 1- DNA (control); Lane 2- DNA+H2O2 (10mM); Lane 3- DNA+H2O2+Ag-AgO-Ag2O nanocomposites (1 µl); Lane 4- DNA+H2O2+Ag-AgO-Ag2O nanocomposites (2 µl); Lane 5- DNA+H2O2+Ag-AgO-Ag2O nanocomposites (3 µl)

Supplementary Files

This is a list of supplementary files associated with this preprint. Click to download.

- floatimage1.png